NUMERICAL MODELING OF GAS STIRRED LADLES

Marcela B. Goldschmit* and A. Heriberto Coppola Owen

Center for Industrial Research, FUDETEC

Córdoba 320, (1054) Buenos Aires, ARGENTINA

* Te: (54) 3489- 435304, e-mail:sidgld@siderca.com

Keywords: turbulence flow, finite element model, gas stirred ladle

Abstract

A finite element analysis of the flow in a gas stirred vessel is presented. Turbulence is modelled using the two equation (*k*-*L*)-predictor / (ε)-corrector scheme algorithm, two alternative studies are compared, with and without flotation in *k*- and ε- transport equations. The biphasic zone is considered as an homogeneus fluid with a reduced density –quasi single phase approach. This reduced density is estimated taking into account the slip velocity between the rising bubbles and the liquid according to correlations from the literature. The numerical results are compared with experimental water model data and then used to predict the flow in two industrial liquid steel ladles with twin excentric Ar injectors.

1. INTRODUCTION

The procedure of stirring the contents of a tank by inert gas injection is used in the metallurgical industry to mix-homogenize the liquid metal inside the ladle[1].

The ladles are near-cylindrical vessels (radius, $R \approx 2 - 3\ m$; height, $H \approx 2 - 4\ m$) that contain liquid steel and a surface slag layer ($0.1 – 0.4\ m$) to avoid the reoxidation of steel. The main processes which take place in the ladle are:

- Addition of alloys (V, Cr, Ti, etc).
- Inductive heating to reach casting temperature($T > 1530\ °C$).
- Inclusion flotation, in order to get them removed by the slag.

All these operations must be carried out while liquid steel is being stirred to allow its chemical and thermal homogenization and to eliminate the possibility of steel solidification close to the ladle walls.

There are two main methods for stirring liquid steel[1]: inert gas injection and electromagnetic stirring. In this work we analyze the first one.

In order to obtain a quick chemical and thermal homogenization and to avoid the reoxidation of the steel due to the top slag layer opening; it is essential to predict where it is convenient to place the gas injection nozzle and to determine the ideal gas flow rate (Q_g).

To predict these characteristics it is necessary to know the fluid velocity[2] via mathematical modeling or physical cold modeling.

The purpose of the present paper is to describe the turbulent recirculatory liquid steel flow in the ladles stirred by gas injection, using a finite element model and our (k-L)-predictor / (ε)-corrector iterative scheme[3-7] to model the turbulent flow.

In Section 2 a brief description of the problem is presented. The empirical equations used to model the gas phase are given in Section 3. The numerical model of turbulent flow is described in Section 4. In the fifth Section we present the comparison between our numerical scheme and an experimental water model from the literature. Finally, an application to an industrial ladle is made in Section 6.

2. GENERAL DESCRIPTION

A general scheme of liquid steel movement caused by injection of inert gas in the ladle is shown in Fig. 1.

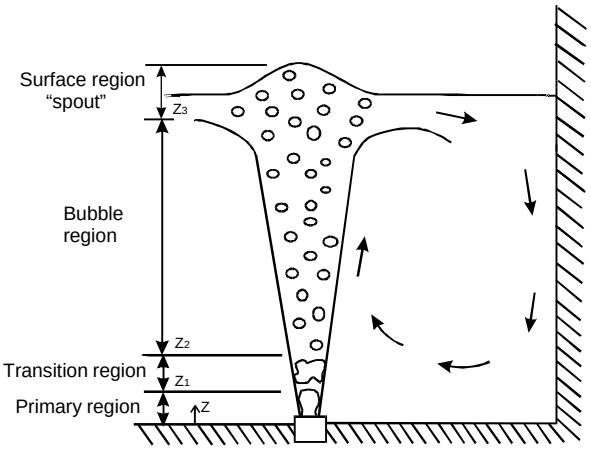

Figure 1. Description of the movement in the process stirred by gas.

Gas is injected into the liquid steel through a porous nozzle where bubbles are formed. The bubbles rising in the liquid break up (disintegrate) into smaller bubbles and coalesce (integrate) into larger bubbles[8]. The liquid steel movement inside the ladle can be characterized by a recirculation zone and a two-phase bubble plume zone[9-12] :

- *Two-phase plume zone*: it is divided in 4 regions with respect to the axial distance from the nozzle exit

  Primary or momentum region: $0 < z < Z_1$, the flow is governed by the inertia force of the injected gas.

  Transition region: $Z_1 < z < Z_2$, the gas loses its kinetic energy and disintegrates in small volumes or bubbles.

  Bubble region: $Z_2 < z < Z_3$, the bubbles rise by the effect of density difference between the gas and liquid steel, until reaching the slag / steel surface.

  Surface region: it is the closest zone to the surface.

- *Recirculation zone*: As the liquid steel flow reaches the surface, the gas bubbles depart from the metal phase and a single phase (liquid steel) recirculation region is formed outside the plume zone. In the upper part of the recirculation zone the liquid steel flows towards the walls. It then flows down along them and finally gets to the ladle bottom.

Two different approaches have been applied to mathematically describe the flow in the gas stirred vessel:

- *Quasi single phase models*[13-17] : where the rising gas-liquid mixture is modeled as a homogeneous fluid, and empirical equations are used to describe the shape and gas hold-up in the plume zone.
- *Two-phase models*[18-20] : these involve the solution of transport equations for variables of each phase (gas and liquid). Turbulence is only modeled in the liquid phase.

The quasi single phase approach is computationally more economical than the two-phase approach. As Mazumdar and Guthrie [2] point out:

- ü Outside the plume region the numerical results of both models are similar and agree satisfactorily with the experimental results.
- ü Whereas inside the plume region the numerical results differ in a slight way. Nevertheless, since in industrial ladles the plume region ocuppies only 3 % of the total volume the results outside the plume are not significantly affected.

Taking into account the economical beneficts and the fact that both models provide acceptable results we use the first approach in this work. In the next Section we will present the empirical equations used to describe the plume zone.

3. CHARACTERISTICS OF THE GAS-LIQUID PLUME

The primary and transition region in the plume occupies a very small volume of the ladle ($Z_2 << H$). Following Koria[12], for argon injected into liquid steel in an industrial ladle, $Z_2 \approx 1$ *to* 3 *mm*. Therefore, the fluiddynamics is mainly controlled by the buoyancy forces made by the gas bubbles[9,21].

The plume is described by its gas fraction (α) and the radius (r_{pl}).

Gas fraction in the plume. Experimental studies show that α has a Gaussian variation with the plume radius and that it can be correlated as a function of a modified Froude number (Fr_m),

$$\alpha = \alpha_{CL} \exp\left[-\ln(2)\left(\frac{r}{b}\right)^2\right] \tag{1}$$

for steel[14,22] :

$$b = 0.28\left(z + H_0\right)^{7/12}\left(\frac{Q_1^{\,2}}{g}\right)^{1/12} \tag{2}$$

$$H_0 = 4.5\sqrt{d_o}\left(\frac{Q_0^{\,2}}{g}\right)^{0.1}$$

for water[23] :

$$b = 0.194\left(\frac{Q_1^{\,2}}{g}\right)^{0.2} Fr_m^{\,-0.129}\left(\frac{z}{d_o}\right)^{0.43} \tag{3}$$

$$Fr_m = \frac{Q_1^{\,2}\,\rho_g}{g\,d_o^{\,5}\left(\rho_l - \rho_g\right)} \approx \frac{Q_1^{\,2}\,\rho_g}{g\,d_o^{\,5}\,\rho_l} \tag{4}$$

where α_{CL} is the centerline gas fraction; b is the radius when $\alpha = \alpha_{CL}/2$; ρ_l and ρ_g are the liquid and gas density [Kg/m^3]; d_o is the injection orifice diameter [m]; $Q_1 = Q_g \frac{T_l}{T_g}\frac{\left(P_{atm}/g\rho_l\right)}{\left[\left(P_{atm}/g\rho_l\right)+H-z\right]}$; $Q_0 = Q_1(z=0)$; Tl and T_g are the liquid and gas temperatures [°K]; P_{atm} is the atmospherically pressure [N/m^2]; and, g is the gravity acceleration [m/s^2].

There are several correlations in the literature for the gas fraction[9,14,17,22-27] .

In this work we estimate α (as a constant in the plume radius and a function of the vertical coordinates) according to the drift flux model[17] which allows for slip between the rising bubbles and the liquid steel as,

$$\alpha = \frac{Q_1 - \pi\, r_{pl}^{\,2}\, \alpha(1-\alpha) U_s}{2\pi \int_0^{r_{pl}} v_{pl}\, r\, dr} \qquad (5)$$

$$v_{pl} = 4.5\, Q_g^{\,0.333}\, H^{0.25}\, R^{-0.25}$$

$$U_s = 1.08 \left(\frac{g\, d_b}{2} \right)^{0.5}$$

for steel[28] :

$$d_b = 0.569 \left(Q_1\, d_o^{\,0.5} \right)^{0.289}$$

for water[29] :

$$d_b = 0.35 \left(Q_g^{\,2} / g \right)^{0.2}$$

where v_{pl} is the plume velocity; U_s is the slip velocity between the bubbles and the liquid; and d_b is the bubbles diameter.

Plume radius. The plume shape is a truncated cone which has a bottom diameter approximately equal to the porous nozzle diameter, and a cone angle given by experimental measurements[9,10,12,14,23,26,30-33].

In this work we use the equivalent plume radius,

$$r_{pl} = 1.5\, b \qquad (6)$$

and b from Equations (2) and (3). A similar approach is used by Mazumdar and Guthrie[17] and Grevet et al.[13].

The liquid steel plume shape is a subject with poor information due to the difficult conditions for measurements and observations, --high temperature, with steel visual opacity and big dimensions of the ladles--. Nevertheless, Mazumdar and Guthrie[16] show that the computational steel flow in the recirculation zone is little dependent on the plume's geometry; for an equivalent gas flow rate a 50 % wider plume will generate a similar recirculating flow in the ladle.

4. NUMERICAL MODELING

In this work the plume zone is treated as a pseudo-one phase with a lower density,

$$\rho = \alpha\ \rho_g + (1-\alpha)\,\rho_l \tag{7}$$

and the recirculation zone is treated as liquid phase, then in this zone $\rho = \rho_l$.

Considering steady state, viscous incompressible flow, constant gas and liquid density, constant laminar viscosity (μ), isothermal flow, buoyancy forces in the plume zone (introducing the term $\rho\ \underline{g}\,\alpha$ in the momentum equations, where α is the time averaged gas fraction) and a turbulence k-ε model, the following equations are solved:

$$\underline{\nabla}.\underline{v} = 0 \tag{8}$$

$$\rho\,\underline{v}.\underline{\nabla v} - \underline{\nabla}.\left[(\mu+\mu^t)\left(\underline{\nabla v}+\underline{\nabla v}^T\right)\right] + \underline{\nabla} P + \rho\ \underline{g}\,\alpha = \underline{0} \tag{9}$$

$$\rho\,\underline{v}.\underline{\nabla} k - \underline{\nabla}.\left[\left(\mu+\frac{\mu^t}{\sigma_k}\right)\underline{\nabla} k\right] - \mu^t\left(\underline{\nabla v}+\underline{\nabla v}^T\right):\underline{\nabla v} + \rho\,\frac{C_\mu k^2}{\mu^t/\rho} - \mu^t\,\underline{g}\ .\underline{\nabla}\alpha = 0 \tag{10}$$

$$\mu^t = C_\mu\,\rho\,\sqrt{k}\,L \tag{11}$$

$$\rho\,\underline{v}.\underline{\nabla}\varepsilon - \underline{\nabla}.\left[\left(\mu+\frac{\mu^t}{\sigma_\varepsilon}\right)\underline{\nabla}\varepsilon\right] - \rho\,C_\mu C_1\,k\left(\underline{\nabla v}+\underline{\nabla v}^T\right):\underline{\nabla v} + \rho\,\frac{C_2\varepsilon^2}{k} - \rho\,C_\mu C_1\,k\,\underline{g}\ .\underline{\nabla}\alpha = 0 \tag{12}$$

$$L = \frac{k^{3/2}}{\varepsilon} \tag{13}$$

where $\underline{v}$ is the time averaged velocity; P is the time averaged pressure; μ^t is the turbulent viscosity; k is the turbulent kinetic energy; ε is the dissipation rate of the turbulent kinetic energy; L is the mixing length; and the values of constants

according to Launder and Spalding[34] are $C_\mu = 0.09$, $C_1 = 1.44$, $C_2 = 1.92$, $\sigma_k = 1.0$, $\sigma_e = 1.0$.

The k-transport equation and ε-transport equation (Eqs. (10) and (12) respectively) are corrected with the inclusion of the last term in each equation, which introduce the bouyancy effect produced by a change of gas fraction in the direction of gravity. The terms $(-\mu^t \, \underline{g} \cdot \underline{\nabla}\alpha)$ and $(-\rho \, C_\mu \, C_1 \, k \, \underline{g} \cdot \underline{\nabla}\alpha)$ were deduced in a similar way to the thermal bouyancy ones presented in Reference 40. As it will be shown in the next Section, the introduction of the bouyancy effect in the *k*- and ε-transport equations establishes a better agreement between our numerical results and the experimental results by Sheng and Irons[35].

An iterative algorithm referred to as (*k*-*L*)-predictor /(ε)-corrector scheme was used to model the quasi-single phase in the ladle. In this iterative scheme a predictor result is obtained using a *k*-*L* model (Eqs. (8-10)) and it is afterwards corrected integrating the ε-transport equation (Eq. (12)). The iterative scheme loops between the predictor and corrector phases until convergence is achieved in L (Eq. (13)). A complete description of the iterative algorithm and the wall boundary condition is shown in our references[3,4] and was implemented by the first author and co-workers in the finite element code FANTOM[42]. The applications of the (*k*-*L*)-predictor /(ε)-corrector turbulence model to the liquid steel movement are shown in Goldschmit et.al.[5-7].

The transport equations (9, 10, 12) are weighted using the Streamline Upwind Petrov Galerkin technique[36] and a standard isoparametric finite element discretization for $\underline{v}$, k and ε (Zienkiewicz et al.[37]).

5. COMPARISON WITH EXPERIMENTAL RESULTS

Results of a water model experiment from Sheng and Irons[35] are used to compare with the numerical algorithm described in Section 2 and 3. The main characteristics are shown in Table 1.

In Figure 2 we show the numerical result with the flotation term in momentum, *k*-transport and ε-transport equations (__); the numerical result with the flotation term only in momentum equation (- - -); and the experimental result from Sheng and Irons[35] (•) at height $z = 0.21\ m$ (half of water height in the vessel). A finite element mesh with 1440 hexahedral elements and 1974 nodes was used to model a 30° portion of the vessel. The correction of *k*- and ε- transport equations with the flotation term show a better approximation to the experimental results.

Table 1. Experimental data from Sheng and Irons[35]

Diameter of ladle (2R)	0.5 m
Water height (H)	0.42 m
Injection orifice diameter	0.004 m
Injection orifice position	Central
Air flowrate	5.0e-5 Nm^3/s
Temperature	ambient
Gas density (ρ_g)	1.17 Kg/m^3
Water density (ρ_l)	996 Kg/m^3
Water viscosity (μ)	10.1E-2 Ns/m^2

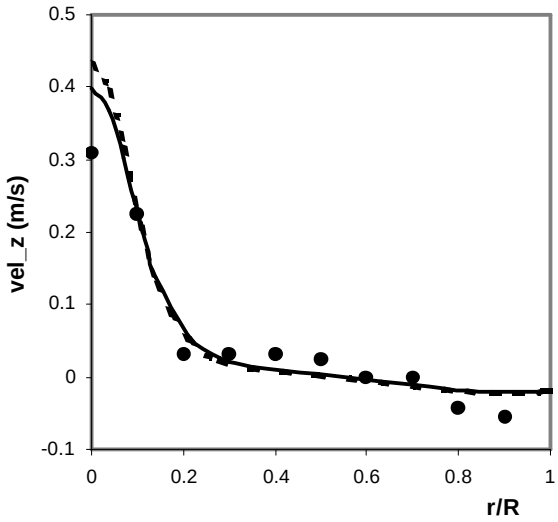

Figure 2. Comparison between experimental results (•) from Sheng and Irons[35] and our numerical results with (__) and without (- -) flotation terms in *k* and ε equations*; z = 0.5 H*

Considering the next set of non-dimensional equations defined by Mazumdar and Guthrie[38], different measurements of velocity fields in water models of gas stirred vessels for a wide range of experimental conditions (see Table 2) present similar non-dimensional results.

$$\underline{v}^* = \frac{\underline{v}}{Q_g / R^2} \tag{14}$$

$$r^* = \frac{r}{R} \tag{15}$$

$$z^* = \frac{z}{H} \tag{16}$$

Table 2. Summary of experimental conditions from literature

References	H [m]	R [m]	Q_g [Nm^3/s]	Gas injection device
Grevet et al.[13]	0.3	0.3	0.0004	Tuyere, 0.0127 m diam.
Sahai et al.[24]	0.45	0.25	0.000413	Submerged lance, 2.16 mm diam.
Mazumdar et.al.[16]	0.93	0.56	0.000667	Submerged lance, 6.3 mm diam.

Johansen et al.[29]	1.237	0.55	0.00061	Porous plug, 50 mm diam.
Anagbo et al.[39]	0.4	0.25	0.0002	Porous plug, 60 mm diam.

In Figure 3 we show these experimental results and our numerical results when flotation is considered in Eqs. (9), (10) and (12) for the experimental data from Johansen and Boysan[29]. A good agreement is observed.

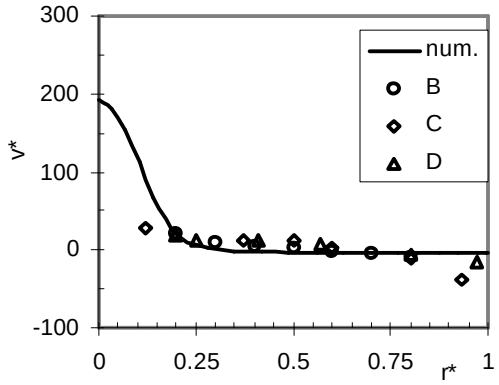

(a) $z^* = 0.2$

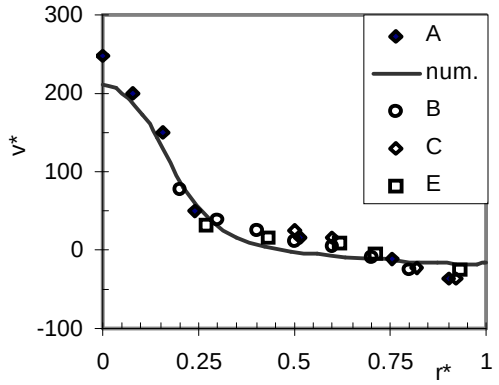

(b) $z^* = 0.5$

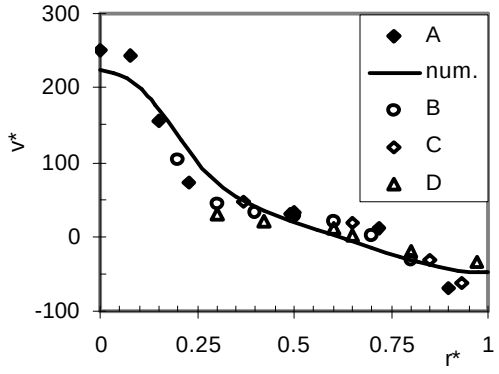

(c) $z^* = 0.8$

Figure 3. Comparison between our numerical results with flotation terms in *k*- and ε-transport equation and experimental results from:

A. Johansen and Boysan[29]
B. Anagbo and Brimacombe[39]
C. Mazumdar and Guthrie[16]
D. Sahai and Guthrie[24]
E. Grevet, Szekely and El Kaddah[13]

Close to the center of the ladle $r^* = 0$ (point to the gas injection) the numerical results show a slight deviation from the experimental results (see Figures 2 and 3), similar differences are shown in the literature[38]. This can be due to an under prediction of turbulence produced by the bubbles; introduced by the assumption of a quasi single phase model in the plume zone. In their work, Sheng and Irons[35], try to amend this differences introducing extra turbulence terms in the k-ε equations so as to match their experimental results. Nevertheless, since our final objective is to deal with an industrial case with liquid steel where experimental information is very scarce we decided to tolerate this difference. Mazumdar and Guthrie[2] show that it is a valid approach because the plume region occupies only 2 or 3 % of the vessel volume and any variations in the numerical velocities within the plume produce only slight variations in the bulk of the liquid.

6. INDUSTRIAL APPLICATIONS

We use our numerical method to model two industrial ladles (named LF1 and LF2) where the liquid steel is stirred with two Ar injections. In Table 3 we show the characteristics of these; the difference between them are the angle and the position of the Ar injection nozzles,

Table 3. Industrial ladle furnace

	LF1	LF2
Bottom diameter, [m]	3.3	3.3
Top diameter, [m]	3.5	3.5
Liquid steel height, [m]	3.5	3.5
Number of porous plug	2	2
Porous plug diameter, [mm]	112	112
Angle between porous plug	120°	150°
Porous plug position, [r/R]	0.6	0.49
Gas density (ρ_g), [Kg/m^3]	0.26	0.26
Liquid steel density (ρ_l), [Kg/m^3]	7000	7000
Liquid steel viscosity (μ), [Ns/m^2]	6.7e-3	6.7e-3

In figures 4 and 5 we show the velocity distribution of LF1 and LF2 when the Ar flow rate is $Qg = 1000\ lt/min$. In these cases taking into account symmetry we modeled only half of the ladle furnace. We observed the difference in the flow patterns when the position of Ar injection nozzles was changed.

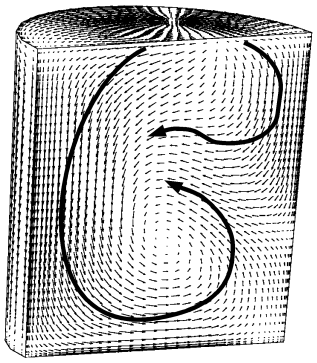

Figure 4. Velocity distribution of LF1,
4179 nodes, 3600 hexahedral elements

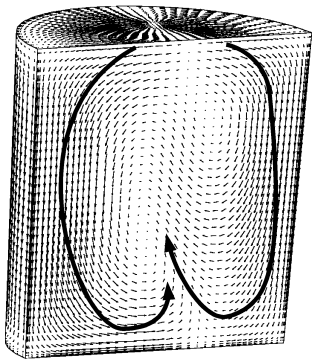

Figure 5. Velocity distribution of LF2,
5019 nodes, 4360 hexahedral elements

In LF1, with a 120° angle between the injectors, the flow forms one main circulation loop that reaches the bottom of the ladle and a second one that only goes half way down the vessel's wall. In LF2 as the angle is raised to 150° the flow on both sides of the plume becomes similar.

The liquid recirculation rate is defined by Turkoglu and Farouk[19] as the total amount of liquid flowing upward or downward through the horizontal mid-plane ($z^* = 0.5$). In Figure 6 we plotted the recirculation flow rate for LF1 and LF2 ladle furnaces against the gas flow rate in each injection of Ar. LF1 presents a greater mixing intensity than LF2.

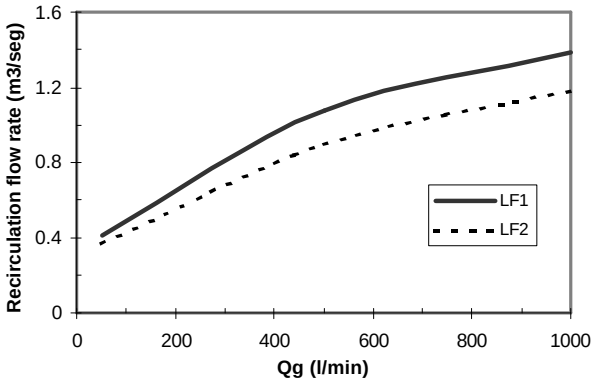

Figure 6. Variation of the recirculation flow rate as a function of gas flow rate.

To analyze the dead volume in the vessel we plotted the volume percentage that has velocities lower than the velocity modules indicated in the abscise axes of the Figure 7. For example: for LF1 and *Q = 1000 lt/min*, the *50 %* of vessel volume has velocities lower than *0.3 m/s*.We observe that the LF1 has less dead volume than LF2 for both gas flow rate analyzed.

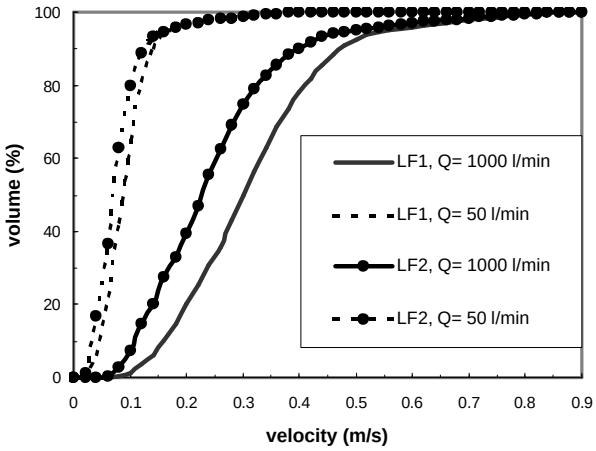

Figure 7. Fraction of the ladle volume under a certain velocity

7. CONCLUSIONS

A numerical analysis by a finite element *k*-ε turbulent model used to obtain design criteria for different gas injection positions in the vessel is presented, with the following characteristics:

- Quasi single phase to model bi-phasic region.
- Gas fraction (α) and plume radius (r_{pl}) from literature.
- (*k*-*L*)-predictor /(ε)- corrector scheme to model turbulence flow.
- Wall law as the boundary conditions at the vessel walls.

- Flotation term in momentum equation.
- Flotation term in *k*- and ε- transport equations (introduced in this work).

When comparing our numerical results with experimental water model results from the literature a good agreement is obtained.

An industrial example of a steelmaking vessel is presented. The numerical model is used to determine the most convenient position for the inert gas injections (generally Ar) in the liquid steel vessel so as to improve mixing.

Numerical results show that slight variations in the position of the gas injectors lead to significant changes in the flow inside the vessel. A better understanding of the fluid dynamics then seems necessary so as to optimize the mixing process. Since experimental studies in the real operating conditions are difficult and expensive and water models show limitations as a predictive tool[40] numerical modeling of the flow turns out to be a promising way of dealing with the problem.

ACKNOWLEDGEMENTS

The authors would like to thank Dr. E.N. Dvorkin for his continuous support in numerical methods. This research was supported by SIDOR , Puerto Ordaz, Venezuela and SIDERAR S.A.I.C., San Nicolas, Argentina.

REFERENCES

1. J. SZEKELY: “Fenómenos de Flujo de Fluidos en Procesamiento de Metales”, 1988, Mexico, Ed. Limusa.
2. D. MAZUMDAR and R.I.L. GUTHRIE: *ISIJ International*, 1995, **35**, 1-20.
3. M.B. GOLDSCHMIT and M.A. CAVALIERE: *Applied Mechanics Reviews*, 1995, **48**, N° 11.
4. M.B. GOLDSCHMIT and M.A. CAVALIERE: *Engineering Computations*, 1997, **14**, 4, 441-455.
5. M.B. GOLDSCHMIT and J.R. PRÍNCIPE: in Proc. Conf. Fourth World Congress on Computational Mechanics, Buenos Aires, Argentina, 1998.
6. M.B. GOLDSCHMIT, R.J. PRÍNCIPE and M. KOSLOWSKI: in Proc. Conf. 3rd. European Conference on Continuous Casting, Madrid, Spain, 1998.
7. M.B. GOLDSCHMIT, R.J. PRÍNCIPE and M. KOSLOWSKI: *International Journal for Numerical Methods in Engineering*, 1999, **46**,1505-1519.
8. S. TURKAN and K.W. LANGE: *Steel Research*, 1987, **58**, 414-420.
9. P.E. ANAGBO, J.K. BRIMACOMBE and A.H. CASTILLEJOS: in Proc. Conf Int. Symposium on Ladle Steelmaking and Furnaces, Canada, 1988.
10. M. IGUCHI, K. NOZAWA and Z. MORITA: *ISIJ International*, 1991, **31**, 952-959.
11. M. IGUCHI, T. KONDOH, Z. MORITA, K. NAKAJIMA, K. HANAZAKI, T. UEMURA and F. YAMAMOTO: *Metallurgical Transactions B*, 1995, **26**, 241-247.
12. S.C. KORIA: *Scandinavian Metallurgy*, 1993, **22**, 271-279.
13. J.H. GREVET, J. SZEKELY and N. EL KADDAH: *Int.J. Heat and Mass Transfer*, 1982, **25**, 487-497.
14. Z. ZHANG, Y. XIE and F. OETERS: *Memories et Etudes Scientifiques Revue de Metallurgie*, 1991, 145-158.
15. JOO and R.I.L. GUTHRIE: *Metallurgical and Materials Transactions B*, 1992, **23**, 765-778.

16. D. MAZUMDAR and R.I.L. GUTHRIE: *Metallurgical and Materials Transactions B,* 1985, **16**, 83-90.
17. D. MAZUMDAR and R.I.L. GUTHRIE: *Appl. Mathe. Modelling*, 1993, **17**, 255-262.
18. N.C. MARKATOS: *Ironmaking and Steelmaking*, 1989, **16**, 266-273.
19. H. TURKOGLU and B. FAROUK: *ISIJ International*, 1991, **31**, 12, 1371-1380.
20. O.J. ILEGBUSI, M. IGUCHI, K. NAKAJIMA, M. SANO and M. SAKAMOTO: *Metallurgical and Materials Transactions B*, 1998, **29**, 211-222.
21. M. IGUCHI, H. TOKUNAGA and H. TATEMICHI: *Metallurgical and Materials Transactions B,* 1997, **28**, 1053-1061.
22. Y. XIE and F. OETERS: *Steel Research*, 1994, **65**, 315-319.
23. S. KORIA and S. SINGH: *Steel Research*, 1990, **61**, 287-294.
24. Y. SAHAI and R.I.L. GUTHRIE: *Metallurgical Transactions B*, 1982, **13**, 125-127.
25. D. BALAJI and D. MAZUMDAR: *Steel Research*, 1991, **62**, 16-23.
26. M. IGUCHI, H. KAWABATA, Z. MORITA and K. NAKAJIMA: *Metallurgical and Materials Transactions B,* 1995, **26**, 67-74.
27. M. IGUCHI, M. KAJI and Z. MORITA,: *Metallurgical and Materials Transactions B,* 1998, **29**, 1209-1218.
28. Y. SAHAI and G.R. ST. PIERRE: *Advances in Transport Processes in Metallurgical Systems*, 1992, Ed. Elsevier.
29. S.T. JOHANSEN and F. BOYSAN: *Metallurgical Transactions B*, 1988, **19**, 755-764.
30. A.H. CASTILLEJOS and J.K. BRIMACOMBE: *Scaninject IV*, Sweden, 1986.
31. G.A. KRISHNA MURTHY, A. GOSH and S. MEHROTRA: *Metallurgical and Materials Transactions B,* 1988, **19**, 885-892.
32. KRISHNA MURTHY and S. MEHROTRA: *Metallurgical and Materials Transactions B,* 1989, **20**, 53-59.
33. KRISHNA MURTHY and S. MEHROTRA: *Ironmaking & Steelmaking*, 1992, **19**, 377-389.

34. B.E. LAUNDER and D.B. SPALDING: *Comp. Meth. in Appl. Mech. and Engrg*., 1974, **3**, 269-289.
35. Y.Y. SHENG and G.A. IRONS: *Metallurgical and Materials Transactions B,* 1993, **24**, 695-705.
36. A.N. BROOKS and T.J.R. HUGHES: *Comp. Meth. Appl. Mech. Engrg*., 1982, **32**, 199-259.
37. O.C. ZIENKIEWICZ and R.L. TAYLOR: "The finite element method", Fourth edition, 1989, Mc Graw Hill, London.
38. D. MAZUMDAR and R.I.L. GUTHRIE: *Steel Research*, 1993, **64**, 6, 286-291.
39. P.E. ANAGBO and J.K. BRIMACOMBE: *Metallurgical Transactions B,* 1990, **21**, 637-648.
40. O.J. ILEGBUSI and J. SZEKELY: *ISIJ International*, 1990, **30**, 731-739.
41. W. Rodi: 'Turbulence models and their application in hydraulics. A state of the art review', Report International Association for Hydraulic Research, The Netherlands, 1980.
42. FANTOM, user manual: International Center for Numerical Methods in Engineering, Barcelona, Spain.